Supporting information

Novel multi-walled carbon nanotubes decorated with gold nanoparticles graft poly(2-methacryloyloxyethyl ferrocenecarboxylate) organic-inorganic nanohybrids: Preparation, characterization and electrochemical sensing applications

Xue-Peng Wei[1ξ], Rui-Qian Zhang[1ξ], Le-Bin Wang[2], Yan-Ling Luo[1]*, Feng Xu[1]*, Ya-Shao Chen[1]

[1] Key Laboratory of Macromolecular Science of Shaanxi Province, School of Chemistry and Chemical Engineering, Shaanxi Normal University, Xi'an 710062, P. R. China

[2] School of Materials Chemistry, Xiangtan University, Xiangtan 411105, P. R. China

ξ Xue-Peng Wei and Rui-Qian Zhang contribute equally to this work.

* Corresponding authors' details:

Yan-Ling Luo and Feng Xu

Fax: +86 29 81530727.

E-mail addresses: luoyanl@snnu.edu.cn (Y. L. Luo) and fengxu@snnu.edu.cn (F. Xu).

Affiliation: Key Laboratory of Macromolecular Science of Shaanxi Province, School of Chemistry & Chemical Engineering, Shaanxi Normal University, Xi'an 710062, People's Republic of China.

1. Modification of MWCNTs

Considering the hydrophobicity of MWCNTs, modification was performed so as to enlarge the micropores on the tube wall of MWCNTs, and thus improve the loading efficiency of Au NPs on the surface of MWCNTs in aqueous phase. Common modification methods include concentrated HNO_3, concentrated H_2SO_4, mixed acid, strong oxidizing H_2O_2, $KMnO_4$, thiophenol and HF etc. Researches manifested that modification of MWCNTs by thiophenol and HF could form C-S and C-F bonds and thus achieved better modification effect. In this study, HF was used to modify MWCNTs, and details were as follows: 0.2 g MWCNTs was dispersed in 40 ml acetone, and rinsed through ultrasonication for about 30-60 min, and then vacuum filtrated and dried under vacuum at 80 °C for 24 h. The modified MWCNTs was ultrasonicated for about 30-60 min in 1.0 mol l^{-1} NaOH aqueous solution and immersed for 5 h. The modified MWCNTs solution was vacuum filtrated, and then rinsed with deionized water until neutrality, and finally dried under vacuum at 80 °C for 24 h. The final product was obtained by ultrasonicating for ca 30 min in a 50 ml 5*wt*% HF solution and then continuously immersing for 8 h with stirring, vacuum filtrating, and then rinsing with deionized water until neutrality, and finally dried under vacuum at 80 °C for 24 h.

2. Preparation of MWCNTs@Au nanocomposites

Preparation of MWCNTs@Au nanocomposites was performed as per an *in situ* reduction method at a mass ratio of MWCNTs to Au of 1:1, 1:2 and 1:4 (*w/w*). Unless otherwise specified, the amount of Au was calculated according to the mass percentage of Au in $HAuCl_4 \cdot 3H_2O$ (ca 48%) thereinafter. In detail, the modified MWCNTs of 0.05 g were dispersed in 92 ml deionized water in a 250 ml beaker, and ultrasonicated for about 1 h. Afterwards, 10 ml 1% (0.25 mmol) $HAuCl_4 \cdot 3H_2O$ aqueous solution at MWCNTs:Au=1:1 (*w/w*) and 5 ml 0.05 M (0.25 mmol) TCD aqueous solution at

Au:TCD:$NaBH_4$=1:1:1.2 (mole ratios) were added into the MWCNTs dispersion. After 3 ml 0.1 M $NaBH_4$ (0.3 mmol) aqueous solution was promptly added while stirring, the color of the solution could be observed to quickly turn to burgundy. The reaction proceeded at room temperature for 24 h with stirring. The mixture solution was centrifuged to collect the sediments at substratum, and the solid was dried at 80 °C, affording MWCNTs@Au nanocomposites (*Yield*: 72%; theoretical amount of Au NPs: 0.0353 g, 2.10 mmol g^{-1}). Likewise, MWCNTs@Au nanocomposites with MWCNTs:Au (*w/w*)=1:2 and 1:4 could be prepared in the same way.

3. Preparation and characterization of monomer MAEFc containing ferrocenes

2-Methacryloyloxyethyl ferrocenecarboxylate (MAEFc) was synthesized through the esterification reaction between FCA and HEMA, as shown in Figure S1(a). In detail, 9.2 g FCA (40.0 mmol), 4.88 g DMAP (40.0 mmol) and 5.86 ml HEMA (48.4 mmol) were added into a hermetic 500 ml three-neck flask in sequence, and then completely dissolved in 300 ml dried DCM at a stirring rate of 1500 rpm. The reaction system was charged with nitrogen and kept stirring for about 60 min. Meanwhile, 9.9 g DCC (48.0 mmol) was fully dissolved in 60 ml desiccative DCM in a 200 ml beaker. When the reaction temperature was cooled to 0 °C, the DCC-DCM solution was dropwise added to the reaction flask within about 60 min through constant pressure funnel. After that, the reaction proceeded at 30 °C for 24 h. The reaction mixture was filtered two or three times to completely remove the byproduct, 1,3-dicyclohexylurea (DCU). The filtrates were evaporated via rotary evaporator, and extracted with saturated $NaHCO_3$ solution several times to remove redundant and/or unreacted DMAP, HEMA and FCA, and extracted with deionized water three times to remove the residual saturated $NaHCO_3$ solution. Anhydrous magnesium sulfate was added into the extractant, and then the crude product was let stand for overnight. The suction filtration was performed to

remove anhydrous magnesium sulfate, and the rotary evaporation operation was conducted to get rid of partial solvents. The purified product was obtained through silica gel column chromatography using petroleum ether and ethyl acetate (*v*/*v*=9:1) as developing solvent. The collected orange solution from the first dot was rotarily evaporated and dried in a vacuum oven at 30 °C for 24 h, giving a pure MAEFc (*Mean yield*: 76%).

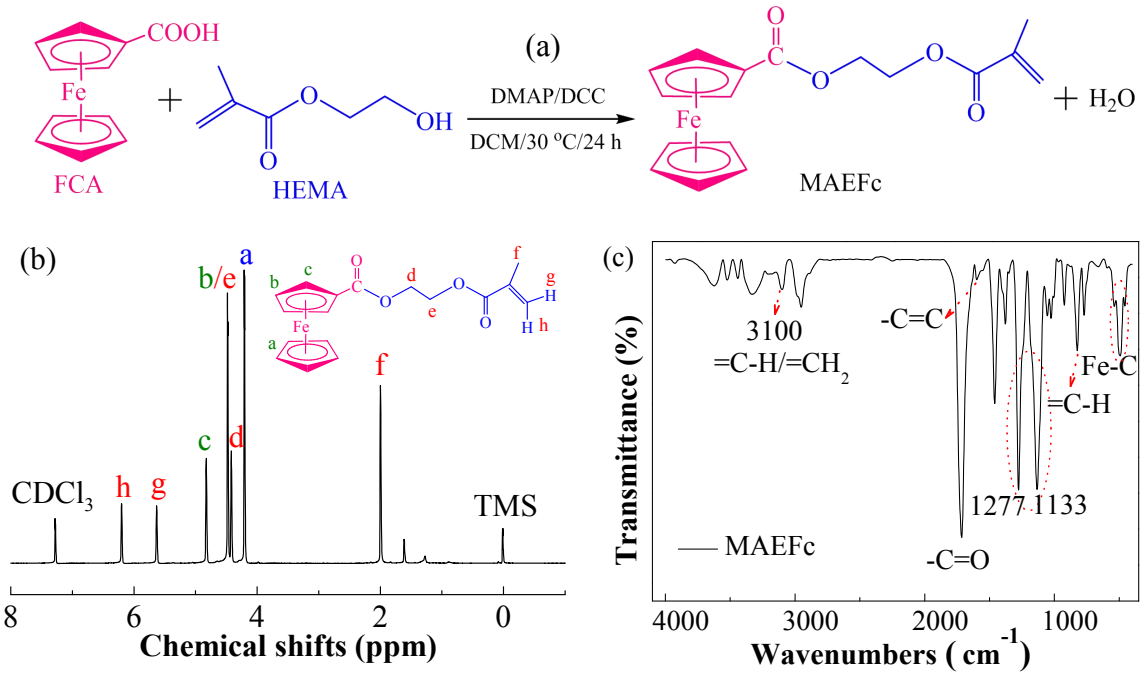

Figure S1 Synthesis scheme (a), ^{1}H NMR in $CDCl_3$ (b) and FTIR spectra (c) of monomer MAEFc containing ferrocenes.

^{1}H NMR spectrum of monomer MAEFc containing ferrocenes is shown in Figure S1(b). The chemical shift signals reflecting ferrocene structural features are located at δ=4.21, 4.48 and 4.82 ppm, which are assigned to the hydrogen proton signals in unsubstituted dicyclopentadienyl rings (5H, *s*, -Cp/-C_5H_5), the proton signals in the *meta*-position (2H, *m*, *m*-C_5H_4) and the *ortho*-position (2H, *m*, *o*-C_5H_4) of monosubstituted dicyclopentadienyl rings, respectively. The methylene proton shift signals near terminal double bonds and close to Cp appear at δ=4.48 (2H, *t*, Cp-OCOCH$_2$-*CH$_2$*OCO-) and 4.42 ppm (2H, *t*, Cp-OCO*CH$_2$*-CH$_2$OCO-), respectively,

where the two signals at δ=4.48 ppm are overlapped corresponding to the above ferrocene and methylene signals. The hydrogen proton resonance signals assigned to the splitting of terminal vinyl groups emerge at δ=5.64 and 6.21 ppm (2H, *d*, -OOC(CH_3)=$\underline{CH_2}$), and the shift signal at δ=2.00 ppm is attributed to the methyl proton shift (3H, *s*, -OOC($\underline{CH_3}$)=CH_2) [1,2]. FTIR spectrum of MAEFc is presented in Figure S1(c). It is noticed that MAEFc produces characteristic vibration bands at 3100 and 772-824 cm^{-1} assigned to the =C-H stretch in Cp rings including terminal double bonds and =C-H bending vibration modes in ferrocene rings; peaks at 2880-2980, 1715, 1600, 1133-1277, 1022-1056 and 457-540 (or 496) cm^{-1} are attributed to the C-H stretch, C=O stretch, C=C stretch, C-O stretch, skeleton characteristic peak of Cp rings and Fe-C or Cp-Fe stretch modes [3], respectively. These findings suggest the successful synthesis of the monomer MAEFc containing ferrocenes.

4. EDX results

EDX results are demonstrated in Figures S2 and S3**.**

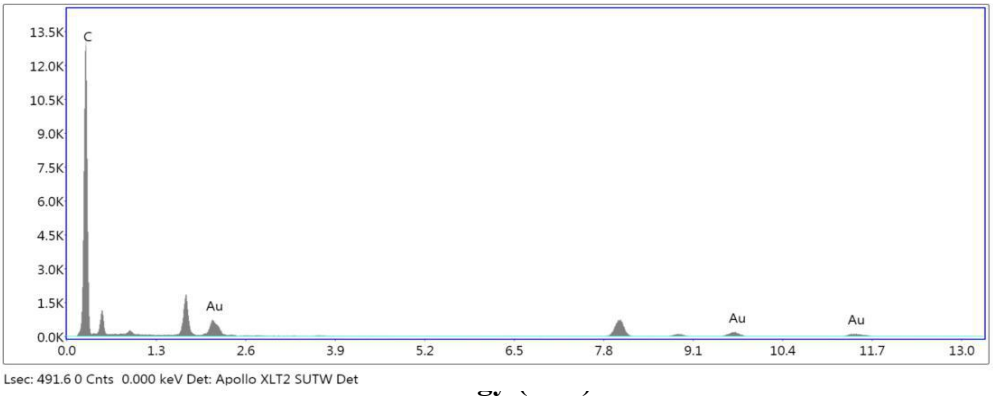

Figure S2 EDX spectrum attached to TEM of MWCNTs@Au nanocomposites.

5. O 1s and C 1s core-level XPS spectra

Figure S4 shows high-resolution XPS spectra of elements C and O in the original pristine MWCNTs, MWCNTs@Au, monomer MAEFc, and MWCNTs@Au-*g*-PMAEFc nanohybrids. The C 1s high-resolution XPS spectrum of

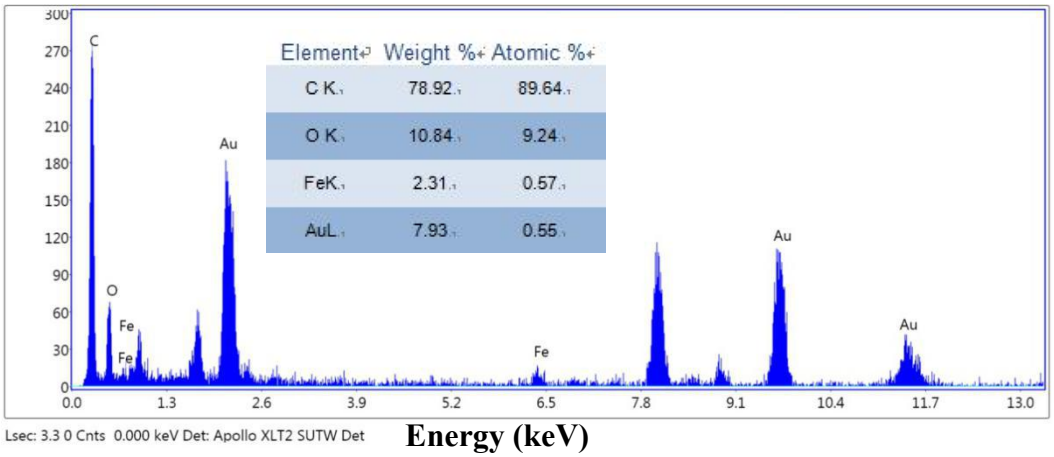

Figure S3 EDX spectrum attached to TEM of MWCNTs@Au-*g*-PMAEFc nanohybrids.

MWCNTs in Figure S4(a) shows the existence of two main signal peaks at BEs of 284.8 and 285.5 eV, which correspond to the sp^2 hybridized carbon atoms in π* conjugated systems (C=C) and sp^3 hybridized C-C bonds at defects and tube structural asymmetry. This indicates that MWCNTs mainly contains element C, reflecting the characteristics of the original MWCNTs [4]. The C 1s high-resolution XPS spectrum in MWCNTs@Au in Figure S4(b) offers four signal peaks at BEs of 284.7, 285.8, 287.0 and 289.2 eV, which separately correspond to the graphene carbon (C=C), C-C single bonds, C-O and -C=O/O=C-O bonds formed by the carbon atoms in MWCNTs and Au NPs sols. Compared with MWCNTs, the emergence of new signals at 287.0 and 289.2 eV and the slight change of BEs at 285.8 eV signify that there exist certain interactions between MWCNTs and Au NPs. The core-level XPS spectrum fitting peak of C 1s orbits in MAEFc is depicted in Figure S4(c). Six kinds of different C elements exist, which have BEs of about 284.2, 284.8, 285.4, 286.2, 287.0 and 288.9 eV corresponding to C=C, C-Fc, C-C, C-O, (R-) C=O and O-C=O, respectively [5-7]. The O 1s core-level spectrum in Figure S4(d) reveals the existence of three kinds of chemically different O species at BEs of about 529.8, 530.9and 531.8 eV, which is assigned to the photoelectronic signals of the O=C, O-C and -O-C=O bonds in

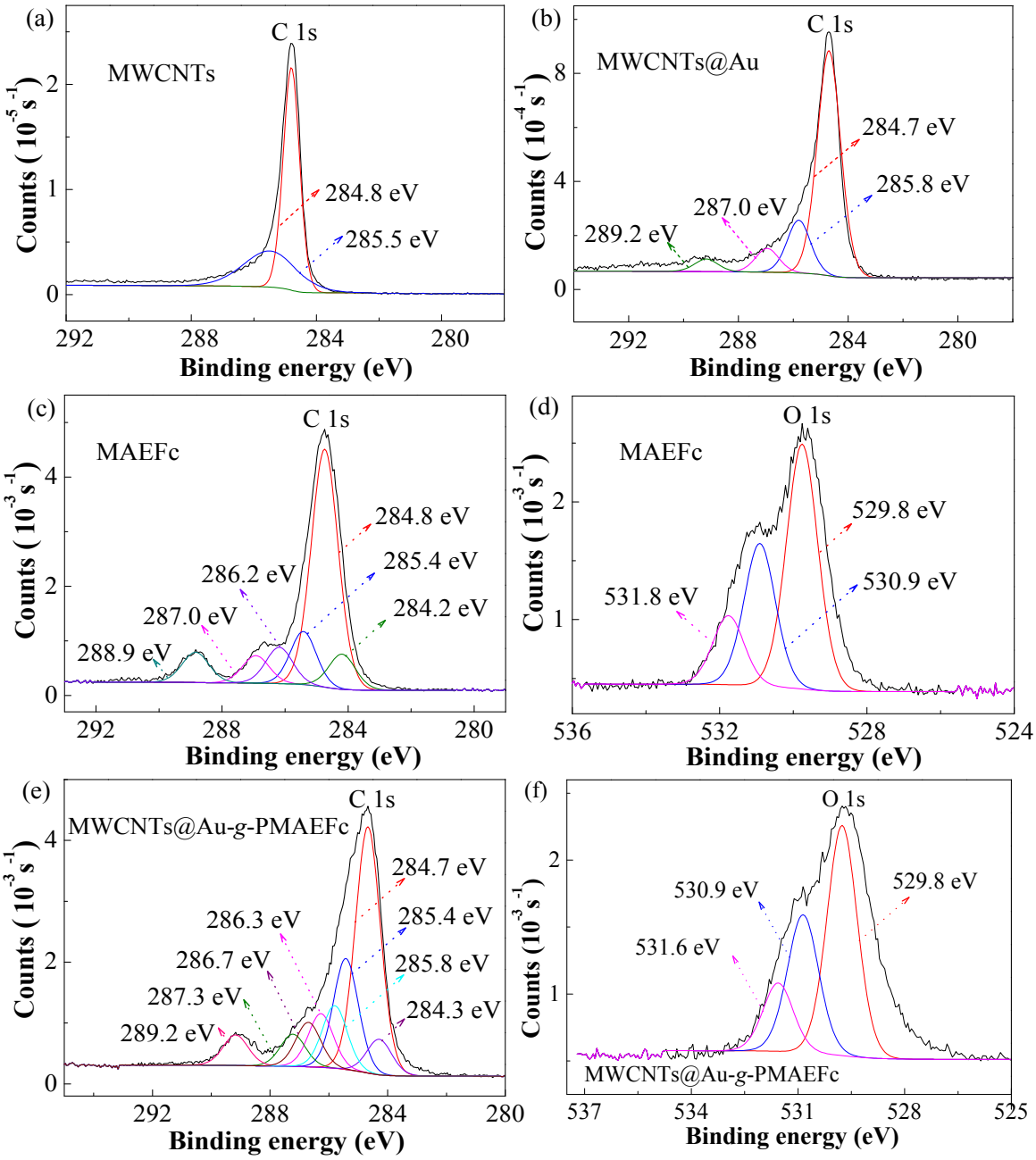

Figure S4 High-resolution XPS spectra of elements C and O: (a) C 1s in the original pristine MWCNTs, (b) C 1s in MWCNTs@Au nanocomposites, (c) C 1s and (d) O 1s in MAEFc, and (e) C 1s and (f) O 1s in MWCNTs@Au-*g*-PMAEFc nanohybrids.

MWCNTs@Au-*g*-PMAEFc [8]. The C 1s core-level spectrum in MWCNTs@Au-*g*-PMAEFc is illustrated in Figure S4(e) (SI). It is noticed that there exist several signal peaks at BEs of 284.3, 284.7, 285.4, 285.8, 286.3, 286.7, 287.3 and 289.2 eV, which correspond to the C=C, ferrocenyl carbons (C-Fe), C-C, C-S, C-O, C-Br, (R-)C=O and O-C=O electronic transition, respectively [9,10]. The O 1s core-level XPS spectra in Figure S4(f) (SI) suggest the presence of three kinds of chemically different O species at BEs of about 529.8, 530.9and 531.7 eV, which is associated with the photoelectronic signals of the O=C, O-C and -O-C=O bonds in MWCNTs@Au-*g*-PMAEFc [8]. These results are in consistent with the C 1s and O 1s XPS spectra in MAEFc in Figures S4(c) and S4(d) (SI), signifying that PMAEFc moieties are grafted onto the surface of MWCNTs or MWCNTs@Au, affording MWCNTs@Au-*g*-PMAEFc organic-inorganic nanohybrids.

6. CV determination

The CV determination results are listed in Table S1.

Table S1 Electrochemical data of the nanohybrids with various composition ratios.

Response type	Curve type	$E_{p,a}$, V	$E_{p,c}$, V	ΔE_p, mV	$I_{p,a}/I_{p,c}$
Au NPs	Curve a	0.04	-0.30	340	1.31
	Curve b	-0.045	-027	225	1.15
	Curve c	-0.05	-0.25	200	0.91
PMAEFc	Curve a	0.20	-0.015	215	1.20
	Curve b	0.19	0.018	172	1.60
	Curve c	0.18	0.03	150	1.07

7. Reproducibility and stability of the modified electrodes

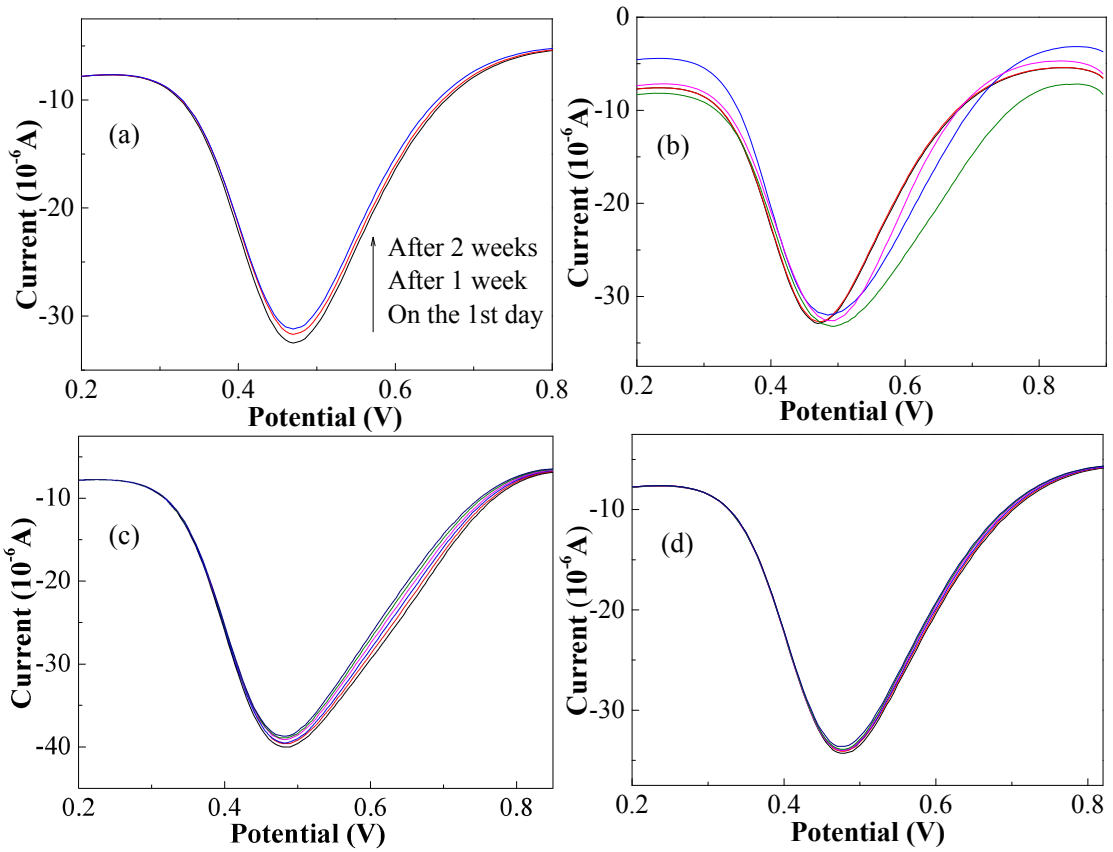

Figure S5 DPV current response in PBS of pH 7.0: (a) with time at trichlorfon concentration of 2.5×10^{-8} mol L^{-1}), (b) determined by five modified electrodes fabricated individually at trichlorfon concentration of 2.5×10^{-8} mol L^{-1}), and by six measurements using the same modified electrode at trichlorfon concentration of (c) 5×10^{-7} amd (d) 5×10^{-8} mol L^{-1}.

8. Detection of trace poisonous and harmful substances

Experimental data of trace trichlorfon residues in real samples are summarized in Table S2 in the next page.

Table S2 Experimental data of trace trichlorfon residues in real samples.

Sample	Added (10^{-8} mol L^{-1})	Found [a] (10^{-8} mol L^{-1})	RSD (%)	Recovery (%)
Apple	1.0	0.92	0.9	92.0
	2.0	1.88	4.3	94.0
	4.0	4.06	2.8	101.5
Tomato	1.0	0.89	0.6	89.0
	2.0	1.96	3.1	98.0
	4.0	3.96	6.4	99.0
Cucumber	1.0	0.87	1.6	87.0
	2.0	1.95	5.1	97.5
	4.0	4.10	3.7	102.5

[a] represents the average value of five measurements.

References

[1] S.G. Zhai, J. Shang, D.Yang, S.Y. Wang, J.H. Hu, G.L. Lu, X.Y. Huang, *J. Polym. Sci. Part A Polym. Chem.,* 2012, 50, 811.

[2] K. Li, J.Q. Zhang, S.Y. Kang, H.M. Shi, H.Y. Zhou, *Chin. J. Appl. Chem.,* 2015, 32, 765.

[3] K. Li, J.Q. Zhang, S.Y. Kang, H.M. Shi, H.Y. Zhou, *Acta Polym. Sin.,* 2015, 2, 236.

[4] X. Wang, H. Yu, F. Liu, M. Li, L. Wan, S. Li, Q. Li, Y. Xu, R. Tian, Z. Yu, D. Xiang, J. Cheng, *Chem. Vapor Deposition,* 2009, 15, 53.

[5] Y. Peng, J.E. Lu, C.P. Deming, L.M. Chen, N. Wang, E.Y. Hirata, S.W. Chen, *Electrochim. Acta,* 2016, 211, 704.

[6] L.P.M. De Leo, E. de la Llave, D. Scherlis, F.J. Williams, *J. Chem. Phys.,* 2013, 138,

114707.

[7] C. Nietzold, P.M. Dietrich, A. Lippitz, T. Gross, W.E.S. Unger, *Surf. Interface Anal.,* 2014, 46, 668.

[8] E.F. Antunes, V.G. de Resende, U.A. Mengui, J.B.M. Cunha, E.J. Corat, M. Massi, *Surf. Sci.,* 2011, 257, 8038.

[9] L.Q. Xu, D. Wan, H.F.F. Gong, K.G. Neoh, E.T. Kang, G.D. Fu, *Langmuir,* 2010, 26, 15376.

[10] M.A. Barakat, A.M. Al-Ansari, R. Kumar, *J. Taiwan Institute Chem. Eng.,* 2016, 63 303.